Thermonuclear Reactions

- Eddington in 1920s hypothesized that fusion reactions between light elements were the energy source of the stars.
- Stellar evolution = (con) sequence of nuclear reactions
- $E_{\text{kinetic}} \approx kT_c \approx 8.62 \times 10^{-8}\, T \sim$ keV,

  but $E_{\text{Coulomb barrier}} = \frac{Z_1 Z_2 e^2}{r} = \frac{1.44\, Z_1 Z_2}{r[\text{fm}]} \sim$ MeV, 3 orders higher than the kinetic energy of the particles.

- Tunneling effect in QM proposed by Gamow (1928, Z. Physik, **52**, 510);
  applied to energy source in stars by Atkinson
  & Houtermans (1929, Z. Physik, **54**, 656)

2

George Gamow (1904-1968)

Russian-born physicist, stellar and big bang nucleosynthesis, CMB, DNA, Mr. Thompkins series

1929 U Copenhagen

1960s U Colorado

3

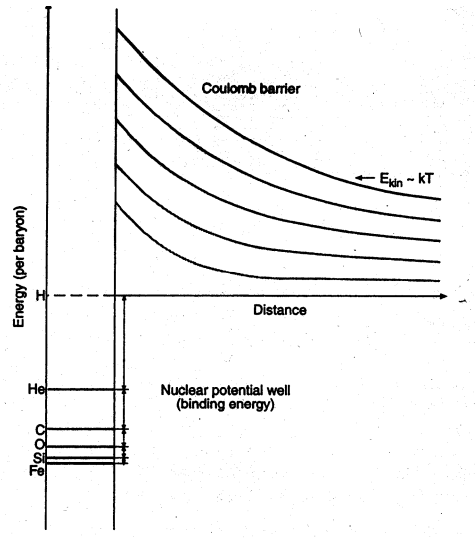

Figure 4.2 Schematic representation of the Coulomb barrier – the repulsive potential encountered by a nucleus in motion relative to another – and the short-range negative potential well that is due to the nuclear force. The height of the barrier and the depth of the well depend on the nuclear charge (atomic number).

4

Quantum mechanics
tunneling effect

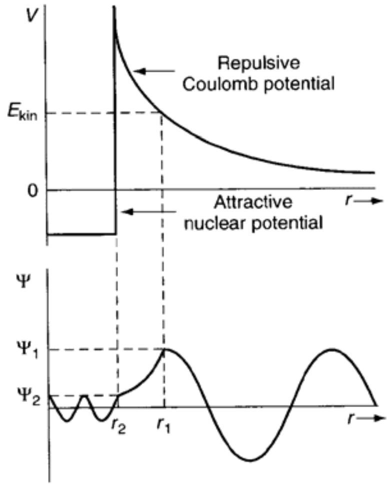

Figure 3.4 Illustration of the potential seen by particle b when approaching particle A with a kinetic energy E_{kin}, and the corresponding wavefunction Ψ; classically, particle b would reach only a distance r_1 from particle A before being repelled by the Coulomb force

5

Cross section for nuclear reactions (penetrating probability)

$$\propto e^{-\pi Z_1 Z_2 e^2/\varepsilon_0 h v}$$

This ↗ as v ↗

Velocity probability distribution (Maxwellian)

$$\propto e^{-mv^2/2kT}$$

This ↘ as v ↗

∴ **Product of these 2 factors ➔ <u>Gamow peak</u>**

6

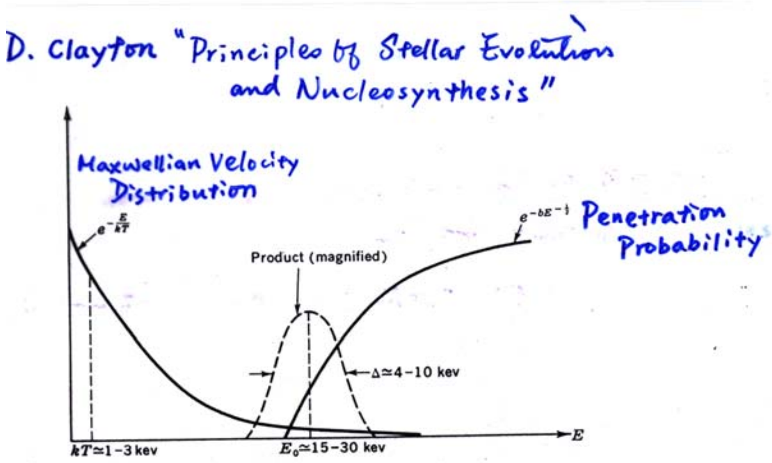

Fig. 4-6 The dominant energy-dependent factors in thermonuclear reactions. Most of the reactions occur in the high-energy tail of the maxwellian energy distribution, which introduces the rapidly falling factor $\exp(-E/kT)$. Penetration through the coulomb barrier introduces the factor $\exp(-bE^{-\frac{1}{2}})$, which vanishes strongly at low energy. Their product is a fairly sharp peak near an energy designated by E_0, which is generally much larger than kT. The peak is pushed out to this energy by the penetration factor, and it is therefore commonly called the *Gamow peak* in honor of the physicist who first studied the penetration through the coulomb barrier.

Clayton 7

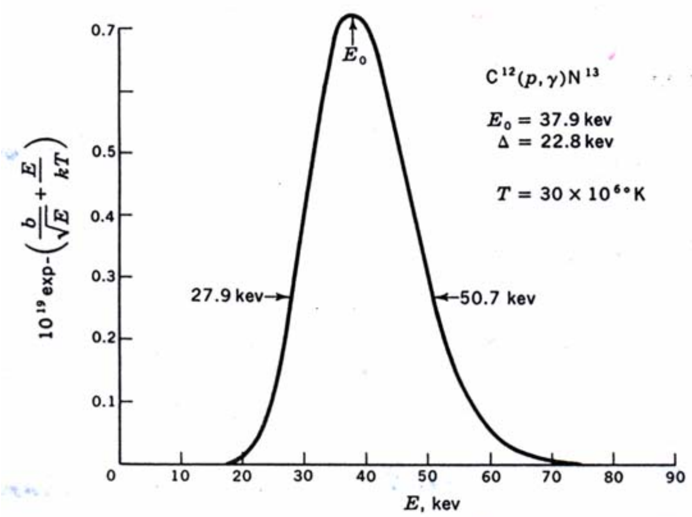

Fig. 4-7 The Gamow peak for the reaction $C^{12}(p,\gamma)N^{13}$ at $T = 30 \times 10^6$ °K. The curve is actually somewhat asymmetric about E_0, but it is nonetheless adequately approximated by a gaussian.

Clayton 8

Resonance → very sharp peak in the reaction rate
→ 'ignition' of a nuclear reaction

Resonance reactions
Energy of interacting particles ≈ Energy level of compound nucleus

So there exists a narrow range of temperature in which the reaction rate ↑↑
→ a power law
→ an ignition (threshold) temperature

For a thermonuclear reaction or a nucleosynthesis (fusion) process, the reaction rate is expressed as

$$q \text{ [energy released per mass]} \propto \rho^m T^n$$

9

Collision

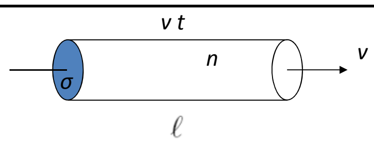

A two-body encounter,
[# of collisions] = [total # of particles in the (moving) volume],
so $N = n\,(\sigma v t)$

✓ **# of collisions per unit time** $= N/t = n\,\sigma v$

✓ **Time between 2 consecutive collisions, mean free time (*N*=1),**
$t_{\text{col}} = 1/\,n\,\sigma v$

✓ **Mean free path** $\ell = v t_{\text{col}} = 1/n\,\sigma$

10

Nuclear reaction rate

- ✓ $r_{12} \propto n_1 n_2 \langle \sigma v \rangle \propto n_1 n_2 \exp\left[-C\left(\frac{z_1^2 z_2^2}{T_6}\right)^{1/3}\right]$ $[\mathrm{cm}^{-3}\mathrm{s}^{-1}]$
- ✓ **As $T \nearrow$, $r_{12} \nearrow \nearrow$**
- ✓ **Major reactions are those with smallest $Z_1 Z_2$**
- ✓ n_i **is the particle volume number density,** $n_i m_i = \rho X_i$, **where** X_i **is the mass fraction**
- ✓ $q_{12} \propto Q\, \rho\, X_1\, X_2 / m_1 m_2$ $[\mathrm{erg\,g^{-1}s^{-1}}]$

11

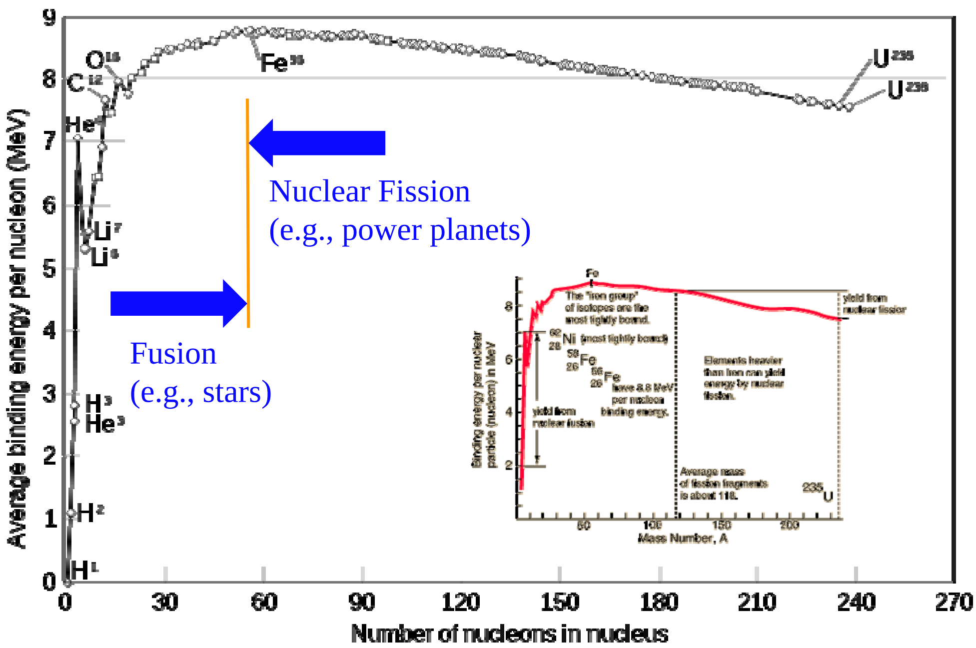

12

Planets — form in circumstellar disks by aggregation of ever larger dust grains (and gas)

Brown dwarfs — form like stars but evolve like planets

In terms of nuclear reactions

- Stars, $M > 0.08\,M_\odot$, core H burning
- BDs, $M > 0.01\,M_\odot$, short D burning — flat $L(t)$ for $t = 10^6 - 10^8$ yr
  - ↳ also for low-mass PMS stars
- Planets, no nuclear burning ever — $L(t)\downarrow$ continuously

13

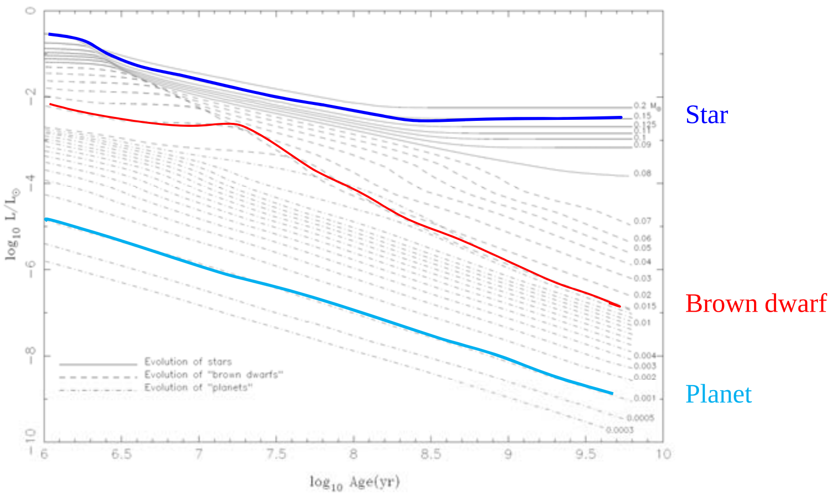

FIG. 7.—Evolution of the luminosity (in $L_\odot$) of solar-metallicity M dwarfs and substellar objects vs. time (in yr) after formation. The stars, "brown dwarfs" and "planets" are shown as solid, dashed, and dot-dashed curves, respectively. In this figure, we arbitrarily designate as "brown dwarfs" those objects that burn deuterium, while we designate those that do not as "planets." The masses (in $M_\odot$) label most of the curves, with the lowest three corresponding to the mass of Saturn, half the mass of Jupiter, and the mass of Jupiter.

Burrows 14

Stars	$\mathcal{M}/M_\odot > 0.08$, core H fusion Spectral types O, B, A, F, G, K, M
Brown Dwarfs	$0.065 > \mathcal{M}/M_\odot > 0.013$, core D fusion $0.080 > \mathcal{M}/M_\odot > 0.065$, core Li fusion Spectral types M6.5–9, L, T, Y Electron degenerate core ✓$10\ \mathrm{g\ cm^{-3}} < \rho_c < 10^3\ \mathrm{g\ cm^{-3}}$ ✓$T_c < 3 \times 10^6$ K
Planets	$\mathcal{M}/M_\odot < 0.013$, no fusion ever

15

THE ASTROPHYSICAL JOURNAL, Vol. **158**, November 1969

THE MASS-RADIUS RELATION FOR COLD SPHERES OF LOW MASS*

H. S. ZAPOLSKY
University of Maryland, College Park, and Center for Theoretical Physics
AND
E. E. SALPETER
Laboratory of Nuclear Studies, Physics Department, and Center for Radiophysics and Space Research, Cornell University, Ithaca, New York
Received 1969 March 14

ABSTRACT

The relationship between mass and radius for zero-temperature spheres is determined for each of a number of chemical elements by using a previously derived equation of state and numerical integration. The maximum radius of a cold sphere is thus found as a function of chemical composition, and a semi-empirical formula for the mass-radius curve is derived.

16

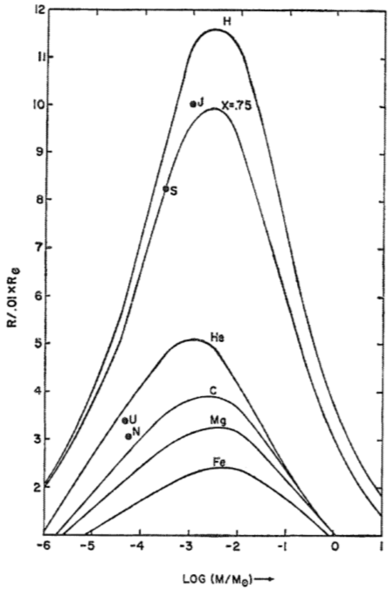

FIG. 1.—Mass-radius plot for homogeneous spheres of various chemical compositions. The points *J*, *S*, *U*, *N* are the observed values for the Jovian planets.

17

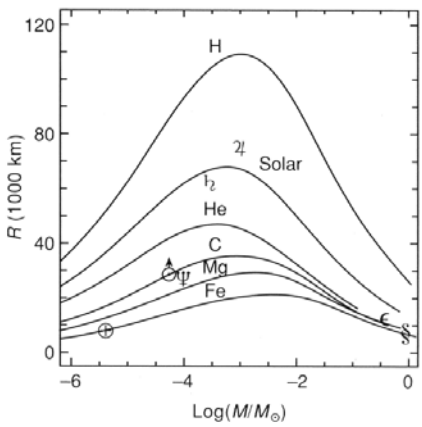

Figure 12.4 Mass-radius relation for low-mass objects (following H. S. Zapolsky & E. E. Salpeter, *Astrophys. J.* 158). Different curves correspond to different compositions, as indicated. The locations of several planets – Earth, Jupiter, Saturn, Uranus and Neptune – are marked by the planets' symbols. Also marked are the locations of two white dwarfs, Sirius B (§) and 40 Eridani B (ϵ) (data from D. Koester (1987), *Astrophys. J.*, 322).

Brown dwarfs and very low-mass stars … partial P_{deg}^{e-}

White dwarfs
≈ completely degenerate,
R↘ as M↗

Terrestrial planets
R ↗ as M↗ ← complicated EoSs

Mass-radius relation max @ $M_{\text{Jupiter}} \approx$ (1/1000) $M_{\odot}$

18

$M_{\odot}c^2 = 2 \times 10^{54}$ ergs
1 amu = 931 Mev/c^2

Deuterium Burning

$$^2H + {}^1H \longrightarrow {}^3He + \gamma \quad (T > 10^6 K)$$

$$^2H({}^1H, \gamma){}^3He$$

$$Q_{DP} = 5.5 \text{ MeV}$$

$$q_{DP} = 4.19 \times 10^7 [D/H] \left(\frac{\rho}{1\, g\, cm^{-3}}\right)\left(\frac{T}{10^6 K}\right)^{11.8} [erg\, g^{-1} s^{-1}]$$

ISM value, $\langle D/H \rangle \sim 2 \times 10^{-5}$

19

$n + p \rightarrow D + \gamma$ (production of D)
$D + D \rightarrow {}^4He + \gamma$ (destruction) → faster

The lower the mass density, the more the D abundant
→ D as a sensitive tracer of the density of the early Universe

Before the Big Bang nucleosynthesis, there were plenty of neutrons, but much less abundant than protons, so all neutrons go into making ^4He

$$\rightarrow {}^4He \approx \frac{n/2}{(n+p)/4} = \frac{2n}{n+p}$$

Current value $n/p \approx 0.12$, so $^4He \approx 2/9$, as observed today.

20

D/H

- 156 ppm … Terrestrial seawater (1.56×10^{-4})
- 22~26 ppm … Jupiter
- 17 ppm … Saturn
- 55 ppm … Uranus
- 200 ppm … Halley's Comet

21

Recall a star's central temperature

$$T_c \sim \frac{\mu G M}{R} \cdot \alpha$$

(α: mass distr.)

Numerically

$$T_c = 7.5 \times 10^6 \, K \left(\frac{M_*}{M_\odot}\right)\left(\frac{R_*}{R_\odot}\right)^{-1}$$

$$\therefore \quad M_* = 0.4 \, M_\odot \longrightarrow T_c \sim 10^6 \, K$$

22

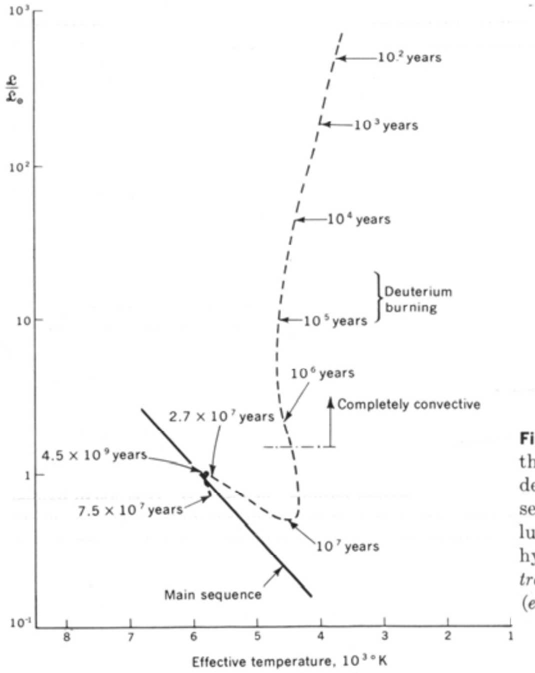

Fig. 5-1 The path on the H-R diagram of the contraction of the sun to the main sequence. The interior has become sufficiently hot to burn deuterium after about 10^5 years. The contraction ceases near the main sequence when the core has become hot enough to replenish the solar luminosity with the thermonuclear power generated by the fusion of hydrogen into helium. [*After D. Ezer and A. G. W. Cameron, The Contraction Phase of Stellar Evolution, in R. F. Stein and A. G. W. Cameron (eds.), "Stellar Evolution," Plenum Press, New York, 1966.*]

Clayton 23

THE ASTROPHYSICAL JOURNAL, **274**:822–829, 1983 November 15

THE BIRTHLINE FOR LOW-MASS STARS

STEVEN W. STAHLER
Harvard-Smithsonian Center for Astrophysics, Cambridge, Massachusetts
Received 1983 January 19; accepted 1983 May 4

ABSTRACT

Using the results of protostar theory, I find the locus in the Hertzsprung-Russell diagram where pre-main-sequence stars of subsolar mass should begin their quasi-static contraction phase and first appear as visible objects. This "birthline" is in striking agreement with observations of T Tauri stars, providing a strong confirmation of the fact that these stars are indeed contracting along Hayashi tracks. The assumption that most T Tauri stars first appear along this line forces a recalibration of their ages. This recalibration removes the puzzling dip in present-day star formation seen in age histograms of several cloud complexes. Since the underlying protostar calculation assumes that the parent cloud was only thermally supported prior to its collapse, the observed location of the birthline places severe restrictions on the degree of extrathermal support provided by rotation, magnetic fields, or turbulence. In addition, the hypothesis that the collapse from thermally supported clouds to low-mass stars proceeds through protostellar disks appears untenable, since the disk accretion process almost certainly produces pre-main-sequence stars with radii well below the observed birthline.

Protostars are heavily embedded in clouds, so obscured, with no definition of $T_{\rm eff}$

Birthline=beginning of PMS; star becomes optically visible ≈ deuterium main sequence

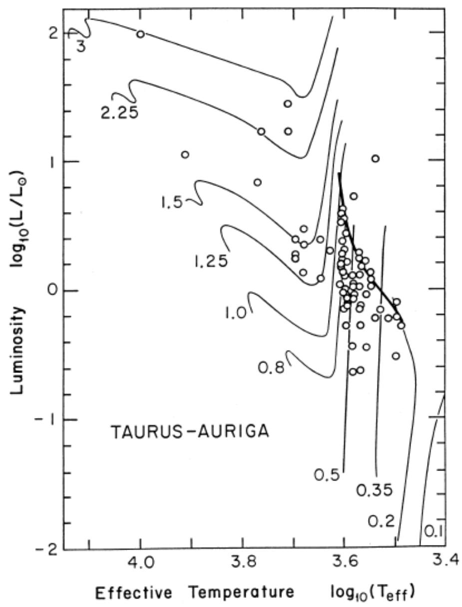

Stahler (1983, 1988), Palla & Stahler (1990)

… compared with observations

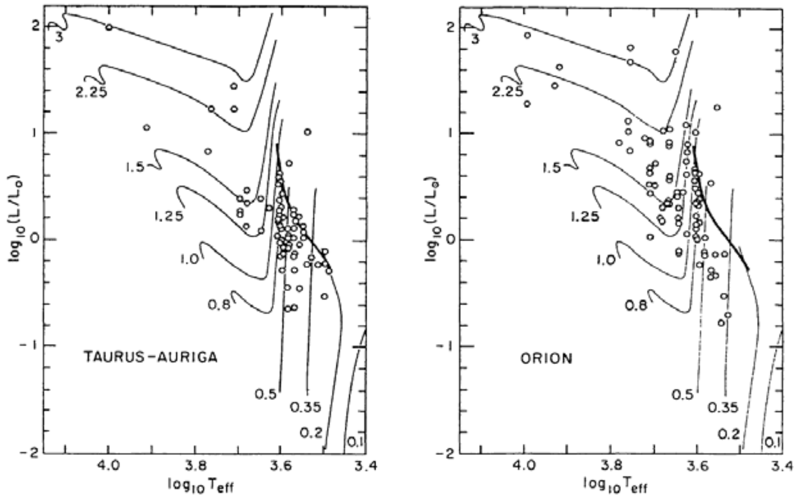

Figure 4 Hertzsprung-Russell diagrams from Cohen & Kuhi (1979) showing theoretical pre-main-sequence contraction tracks and T Tauri stars in the Taurus-Auriga and Orion cloud complexes. The heavy solid curve is the theoretical "birthline" of Stahler (1983).

25

Lithium Burning

$^{7}Li + {}^{1}H \longrightarrow {}^{4}He + {}^{4}He$ ($T > 3 \times 10^{6}$ K)

ISM $[Li/H] \sim 2 \times 10^{-9}$

Primordial abundance 10 x lower,
produced by cosmic rays α hitting 4He
(inverse reaction)

Li measurable in stellar spectra

Li I 6708 Å absorption

(actually doublet 6707.78 and 6707.93
but difficult to resolve

26

Presence of Li I λ6707 absorption → stellar youth

Ca I λ6718 prominent in late-type stars

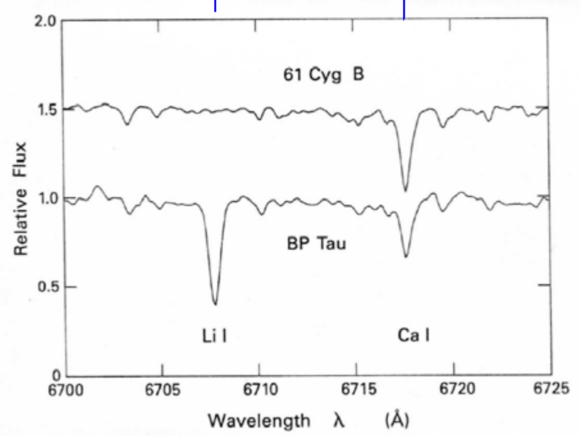

Figure 16.9 Lithium absorption in a pre-main-sequence star. Shown is a portion of the optical spectrum of BP Tau, a T Tauri star of spectral type K7, corresponding to an effective temperature of 4000 K. Also shown, for comparison, is a main-sequence star of the same spectral type, 61 Cyg B. Only in the first star do we see the Li I absorption line at 6708 Å. Both objects also have a strong line due to neutral calcium.

Stahler & Palla 27

M > 1.2 M_sun → shallow convection → surface Li does not deplete during contraction

For protostars with $T_c \geq 3 \times 10^6$K, the central lithium is readily destroyed.

Stars $\geq 0.9\, M_{\odot}$ become radiative at the core, so Li not fully depleted.

Li abundance → age clock

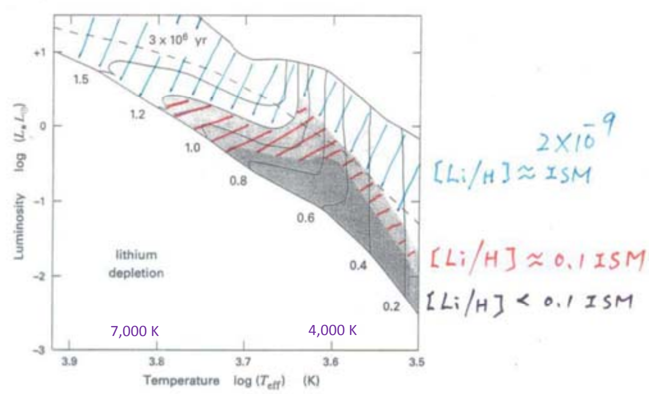

Figure 16.10 Theoretical prediction of pre-main-sequence lithium depletion. Within the white area between the birthline and the ZAMS, the surface [Li/H] is equal to its interstellar value of 2×10^{-9}. Stars in the lightly shaded region have depleted the element down to 0.1 times the interstellar value. The darker shading indicates depletion by at least this amount. Note also the masses on the ZAMS, in solar units, and the indicated isochrone.

Stahler & Palla 28

Older → depletion at higher T_{eff}

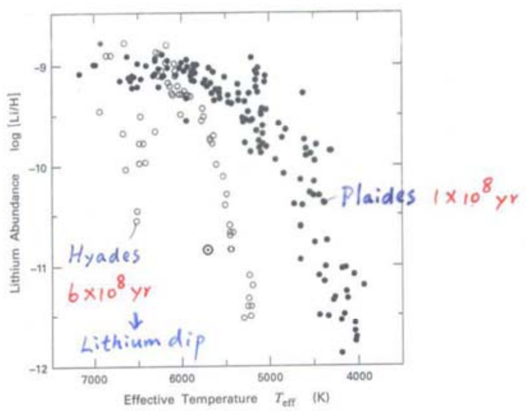

$[Li/H] \downarrow$ as $T_{eff} \downarrow$

Stahler & Palla

29

A hydrogen gas — proton-proton chains

$4\,H \rightarrow {}^4He$ unlikely ⇒ a chain of reactions

baryon #, lepton #, charges all conserved

$p^+ + p^+ \rightarrow {}^2D^+ + e^+ + \nu$ $\langle 1.4\times10^{10}\,yr\rangle$

(1.44 MeV) neutrino → 0.26 MeV escaped

${}^2D + p \rightarrow {}^3He + \gamma$ $\langle 6\,s\rangle$

(5.49 MeV)

${}^3He + {}^3He \rightarrow {}^4He + 2p$ $\langle 10^6\,yr\rangle$

(12.85 MeV) PP I chain

Note: net $6p \rightarrow {}^4He + 2p$

${}^3He + {}^4He \rightarrow {}^7Be + \gamma$

0.420 MeV to the positron and neutrino; position and electron (each 0.511 MeV rest energy) annihilate ➔ 1.442 MeV

... but the nucleus of deuterium, a deuteron, consists of a proton and a neutron!

30

- ✓ $p + p \to {}^2He$ (unstable)$\to p + p$
- ✓ **Hans Bethe (1939) realized that the weak interaction was capable of converting a proton to a neutron (!) first**
- ✓ **Weak interaction → very small cross section**
- ✓ **The neutron is more massive, so this requires energy, i.e., it is an endothermic process, but neutron + proton → deuteron (releasing binding energy, so exothermic)**

31

$^3He + {}^3He \to {}^4He + 2p$ (12.85 MeV) $\langle 10^6\ yr \rangle$

PP I chain

Note: net $6p \to {}^4He + 2p$

$^3He + {}^4He \to {}^7Be + \gamma$

$^7Be + e^- \to {}^7Li + \nu$

$^7Li + p \to 2\,{}^4He$

PP II chain

All 3 branches operate simultaneously.

$^7Be + p^+ \to {}^8B + \gamma$

$^8B \to {}^8Be + e^+ + \nu$

$^8Be \to 2\,{}^4He$

PP III chain

32

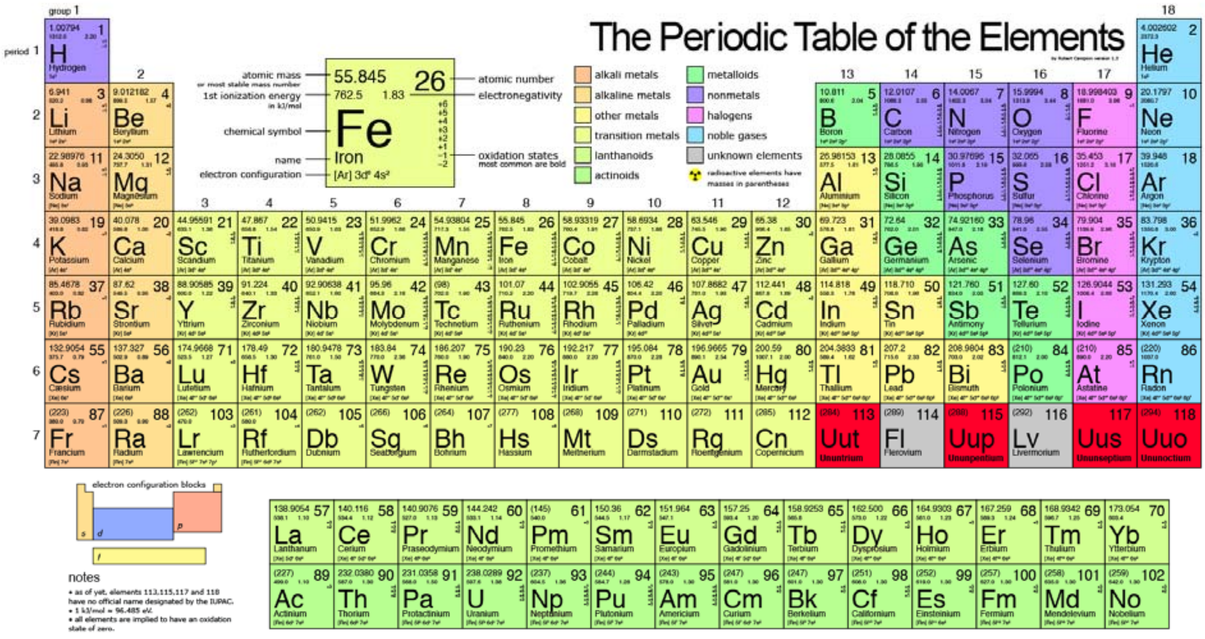

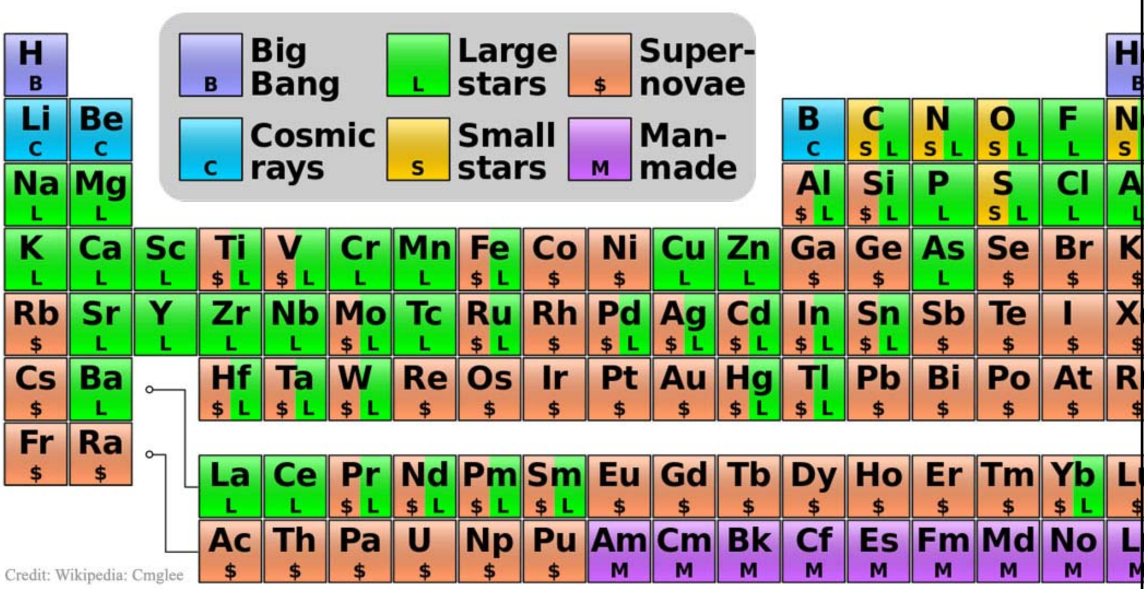

https://apod.nasa.gov/apod/ap160125.html

34

The proton-proton chain

$^1H + {}^1H \to {}^2D + e^+ + \nu_e$ (1.44 MeV, 1.4×10^{10} yr)
$^2D + {}^1H \to {}^3He + \gamma$ (5.49 MeV, 6 s)

pp I important when
$T_c > 5 \times 10^6$K

$Q_{total} = 1.44 \times 2 + 5.49 \times 2 + 12.85 = 27.7$ MeV
$Q_{net} = 27.7 - 0.26 \times 2 = 26.2$ MeV

pp I chain

$^3He + {}^3He \to {}^4He + {}^1H + {}^1H$ (12.85 MeV, 10^6 yr)
Note: net $6\ {}^1H \to {}^4He + 2\ {}^1H$

pp II chain

$^3He + {}^4He \to {}^7Be + \gamma$
$^7Be + e^- \to {}^7Li + \nu_e$
$^7Li + {}^1H \to {}^4He + {}^4He$

pp III chain

$^3He + {}^4He \to {}^7Be + \gamma$
$^7Be + {}^1H \to {}^8B + \gamma$
$^8B + \to {}^8Be + e^+ + \nu_e$
$^8Be \to {}^4He + {}^4He$

The baryon number, lepton number, and charges are all conserved.

All 3 branches operate simultaneously.

pp I is responsible for > 90% stellar luminosity

35

Exercise

Assuming that the solar luminosity if provided by $4\ {}^1H \to {}^4He$, liberating 26.73 MeV, and that the neutrinos carry off about 2% of the total energy. Estimate how many neutrinos are produced each second from the sun? What is the solar neutrino flux at the earth? (How many neutrinos pass through your body per second?)

36

Solution

2% is carried away by neutrinos, so the actual energy produced for radiation

$$E = (0.98 \times 26.731 \text{ MeV}) \times 1.6 \times 10^{-12} \text{ erg/eV}$$

Each alpha particle produced → 2 neutrinos, so with $L_{\odot} = 3.846 \times 10^{33}$ ergs/s, the neutrino production rate is $2 \times 10^{38}\ \nu/\text{s}$, and the flux at earth is $2 \times 10^{38} / 4\pi\ (1\ \text{AU})^2 \approx 6.6 \times 10^{10}\ \nu\ \text{cm}^{-2}\text{s}^{-1}$

37

The thermonuclear reaction rate,

$$r_{pp} = 3.09 \times 10^{-37}\ n_p^2\ T_6^{-2/3} \exp\left(-33.81\ T_6^{-1/3}\right)$$

$$(1 + 0.0123\, T_6^{1/3} + 0.0109\, T_6^{2/3} + 0.0009\, T_6)\quad [\text{cm}^{-3}\text{s}^{-1}],$$

where the factor $3.09 \times 10^{-37}\ n_p^2 = 11.05 \times 10^{10}\ \rho^2 X_H^2$

$$q_{pp} = 2.38 \times 10^{6}\ \rho\ X_H^2\ T_6^{-2/3} \exp\left(-33.81\ T_6^{-1/3}\right)$$

$$(1 + 0.0123\, T_6^{1/3} + 0.0109\, T_6^{2/3} + 0.0009\, T_6)\quad [\text{erg g}^{-1}\text{s}^{-1}]$$

38

PP I vs PP II

i.e., ^3He to react with ^3He lower temp.

or with ^4He $T > 1.4\times10^7 K$

Relative importance of each chain

i.e, branching ratio $\longleftrightarrow T, \rho, \mu$

$T > 3\times10^7 K$, PP III dominates

but in reality, at this temperature, CNO reactions take over.

Overall rate of energy generation is determined by the slowest reaction, i.e, the 1st one, $\tau \sim 10^{10}$ yr

$\varepsilon_{pp} \sim \rho^1 T^n$, $n \sim 4-6$

$Q_{pp} \sim 26.73$ MeV ≈ 6.54 MeV per proton

$n \sim 6$ for $T \approx 5\times10^6$ K
$n \sim 3.8$ for $T \approx 15\times10^6$ K (Sun)
$n \sim 3.5$ for $T \approx 20\times10^6$ K

39

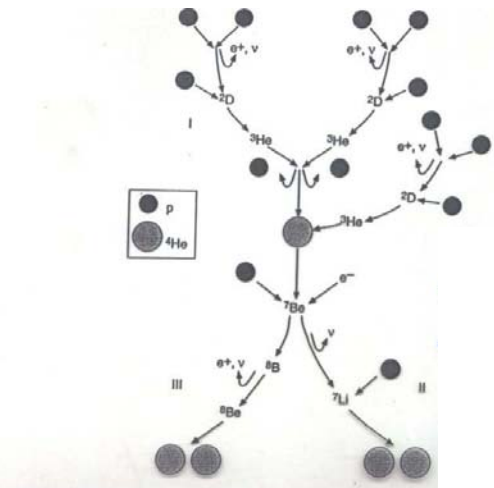

Figure 4.3 The nuclear reactions of the p–p I, II, and III chains.

Among all fusion processes, the p-p chain has the lower temperature threshold, and the weakest temperature dependence.

$Q_{pp} = (M_{4H} - M_{He})\, c^2$
$= 26.73$ MeV

But some energy (up to a few MeV) is carried away by neutrinos.

40

CNO cycle (bi-cycle)   C, N, O as catalysts

$^{12}C + {}^{1}H \rightarrow {}^{13}N + \gamma$ 10^6 y $^{14}N + {}^{1}H \rightarrow {}^{15}O + \gamma$

$^{13}N \rightarrow {}^{13}C + e^+ + \nu$ 14 min $^{15}O \rightarrow {}^{15}N + e^+ + \nu$

$^{13}C + {}^{1}H \rightarrow {}^{14}N + \gamma$ 3×10^5 y $^{15}N + {}^{1}H \rightarrow {}^{16}O + \gamma$ ←

$^{14}N + {}^{1}H \rightarrow {}^{15}O + \gamma$ 3×10^8 y $^{16}O + {}^{1}H \rightarrow {}^{17}F + \gamma$

$^{15}O \rightarrow {}^{15}N + e^+ + \nu$ 82 s $^{17}F \rightarrow {}^{17}O + e^+ + \nu$

→ $^{15}N + {}^{1}H \rightarrow {}^{12}C + {}^{4}He$ 10^4 y $^{17}O + {}^{1}H \rightarrow {}^{14}N + {}^{4}He$

CN cycle more significant

NO cycle efficient only when $T > 20 \times 10^6$ K

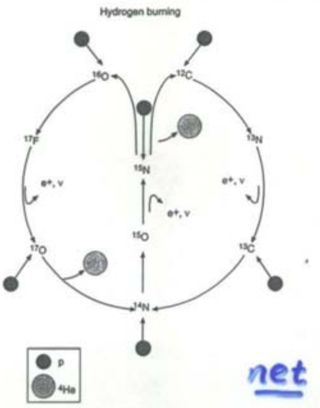

Figure 4.4 The nuclear reactions of the CNO bi-cycle.

Recognized by Bethe and independently by von Weizsäcker

CN cycle + NO cycle

Cycle can start from any reaction as long as the involved isotope is present.

net $4H \rightarrow {}^{4}He$

$Q_{CNO} \sim 25$ MeV
after that carried away by the neutrinos

$\varepsilon_{CNO} \sim \rho T^{16}$

41

表 6.2 氢燃烧的核反应

序号 r	反应式	Q.(MeV)	$(q_\nu)_r$(MeV)	速率 $N_A\langle\sigma v\rangle$ ($cm^3 mol^{-1} s^{-1}$)
1	$^{1}H(p,e^+\nu)^{2}H$	1.442	0.265	1.26×10^{-20}
2	$^{2}H(p,\gamma)^{3}He$	5.494		1.85×10^{-3}
3	$^{3}He(^{3}He,2p)^{4}He$	12.860		2.29×10^{-13}
4	$^{3}He(\alpha,\gamma)^{7}Be$	1.588		1.67×10^{-18}
5	$^{7}Be(e^-,\nu)^{7}Li$	0.862	0.862	* 4.59×10^{6} s
6	$^{7}Li(p,\gamma)^{8}Be(\alpha)^{4}He$	17.346		3.21×10^{-11}
7	$^{7}Be(p,\gamma)^{8}B$	0.137		1.38×10^{-14}
8	$^{8}B(e^+\nu)^{8}Be(\alpha)^{4}He$	18.072	6.710	* 0.77s
9	$^{12}C(p,\gamma)^{13}N$	1.944		1.26×10^{-12}
10	$^{13}N(e^+\nu)^{13}C$	2.221		* 870s
11	$^{13}C(p,\gamma)^{14}N$	7.551		4.59×10^{-12}
12	$^{14}N(p,\gamma)^{15}O$	7.297		1.30×10^{-14}
13	$^{15}O(e^+\nu)^{15}N$	2.754	0.9965	* 178s
14	$^{15}N(p,\alpha)^{12}C$	4.966		3.62×10^{-10}
15	$^{15}N(p,\gamma)^{16}O$	12.128		2.76×10^{-13}
16	$^{16}O(p,\gamma)^{17}F$	0.600		2.51×10^{-16}
17	$^{17}F(e^+\nu)^{17}O$	2.762	0.9994	* 95s
18	$^{17}O(p,\alpha)^{14}N$	1.191		4.07×10^{-16}
19	$^{17}O(p,\gamma)^{18}F$	5.607		3.05×10^{-16}
20	$^{18}F(e^+\nu)^{18}O$	1.655	0.3965	* 1.67s
21	$^{18}O(p,\alpha)^{15}N$	3.980		7.63×10^{-13}
22	$^{18}O(p,\gamma)^{19}F$	7.994		8.43×10^{-16}
23	$^{19}F(p,\alpha)^{16}O$	8.114		6.25×10^{-15}

* 表示 β 衰变的半周期.

(根据 Caughlan and Fowler, 1988; Harris, et al. 1983; Fowler, et al., 1975; 弱相互作用过程的快慢用原子半衰期表示，根据 Fuller, et al., 1980, 1982, 1985; Clayton, 1968). 表中的速率为典型温度下的速率，p—p 链的典型温度为 1×10^7 K, CNO 循环的典型温度为 2.5×10^7 K.

Huang 42

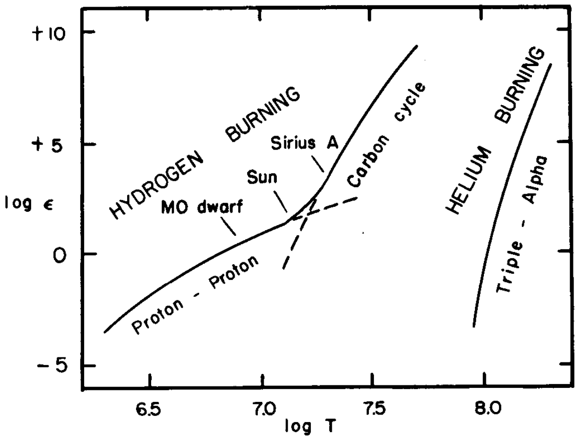

Fig. 10.1. Nuclear energy generation as a function of temperature (with $\rho X^2 = 100$ and $X_{CN} = 0.005X$ for the proton-proton reaction and the carbon cycle, but $\rho^2 Y^3 = 10^8$ for the triple-alpha process).

Schwarzschild

At the center of the Sun,
$q_{\mathrm{CNO}}/q_{\mathrm{pp}} \approx 0.1$

CNO dominates in stars $> 1.2\ M_\odot$, i.e., of a spectral type F7 or earlier
→ large energy outflux
➔ a convective core

This separates the lower and upper MS.

CN cycle takes over the PP chains near T_6=18.
Helium burning starts ~10^8 K.

43

The Solar Standard Model (SSM)

Best structural and evolutionary model to reproduce the observational properties of the Sun

- $L_\odot = 3.842 \times 10^{33}$ [ergs/s]
- $R_\odot = 6.9599 \times 10^{10}$ [cm]
- $M_\odot = 1.9891 \times 10^{33}$ [gm]
- Spectroscopic observations → Z/X =0.0245
  (latest value seems to indicate $Z_\odot = 0.013$)

Neglecting rotation, magnetic fields, and mass loss ($dM/dt \sim 10^{-14}\ M_\odot$/yr)

Sun Fact Sheet
http://nssdc.gsfc.nasa.gov/planetary/factsheet/sunfact.html

44

A He Gas — the triple-alpha process

He-burning ignites at Tc ~ 10^8 K

$^4He + ^4He \rightarrow ^8Be$ (−95 keV, i.e., endothermic)

The lifetime of ^{8}Be is 2.6×10^{-16} s but is still longer than the mean-free time between α particles at T_8 (Edwin Salpeter, 1952)

$^8Be + ^4He \rightarrow ^{12}C + \gamma$ (7.4 MeV) ← bottleneck

Note: net $3\ ^4He \rightarrow ^{12}C$

$Q_{3\alpha} = 7.275$ MeV net $3\ ^4He \rightarrow ^{12}C$

↪ 5.8×10^{17} erg g^{-1} ~ 0.1 of H → He

$\varepsilon_{3\alpha} \sim \rho^2 T^{40}$ ∵ bottleneck = 2nd reaction ↔ ^{8}Be

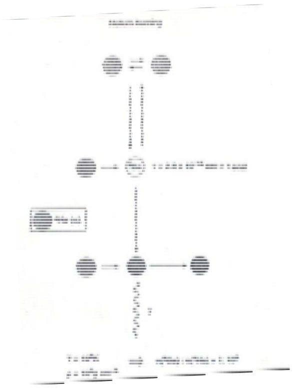

Nucleosynthesis during helium burning

$C^{12}(\alpha, \gamma) O^{16}$ Q = 7.162 MeV

$O^{16}(\alpha, \gamma) Ne^{20}$

A succession of (α, γ) processes

→ $^{16}O, ^{20}Ne, ^{24}Mg$ … (the α-process)

A carbon/oxygen Gas

$^{12}C + ^{12}C$

$T \gtrsim 5 \times 10^8$ K

$Q_{cc} \sim 13$ MeV

$^{12}C + ^{12}C \rightarrow ^{24}Mg + \gamma$
$\rightarrow ^{23}Mg + n$
$\rightarrow ^{23}Na + p$
$\rightarrow ^{20}Ne + \alpha$
$\rightarrow ^{16}O + 2\alpha$

$^{16}O + ^{16}O \rightarrow ^{32}S + \gamma$
$\rightarrow ^{31}S + n$
$\rightarrow ^{31}P + p$
$\rightarrow ^{28}Si + \alpha$
$\rightarrow ^{24}Mg + 2\alpha$

$^{16}O + ^{16}O$

$T \gtrsim 10^9$ K

$Q_{OO} \sim 16$ MeV

C-burning ignites when Tc ~ (0.3-1.2) × 10^9 K, i.e., for stars 15-30 $M_\odot$

O-burning ignites when Tc ~ (1.5-2.6) × 10^9 K, i.e., for stars > 15-30 $M_\odot$

The p and α particles produced are captured immediately (because of the low Coulomb barriers) by heavy elements

➔ isotopes

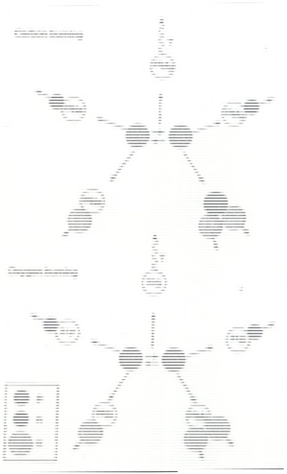

O burning → Si

46

$$q_{PP} = 2.4 \times 10^6 \, \rho \, X^2 \, T_6{}^{-2/3} \exp\left[-33.8 \, T_6{}^{-1/3}\right] \quad [\mathrm{erg \, g^{-1} \, s^{-1}}]$$

$$q \propto \rho \, X_H^2 \, T^4$$

$$q_{CN} = 8 \times 10^{27} \, \rho \, X \, X_{CN} \, T_6{}^{-2/3} \exp\left[-152.3 \, T_6{}^{-1/3}\right] \quad [\mathrm{erg \, g^{-1} \, s^{-1}}]$$

$$q \propto \rho \, X_H X_{CN} \, T^{16}$$

$$\frac{X_{CN}}{X_H} = 0.02 \text{ ok for Pop I}$$

$$q_{3\alpha} = 3.9 \times 10^{11} \, \rho^2 X_\alpha{}^3 \, T_8{}^{-3} \exp[-42.9 \, T_8] \quad [\mathrm{erg \, g^{-1} \, s^{-1}}]$$
$$\approx 4.4 \times 10^{-8} \, \rho^2 X_\alpha{}^3 \, T_8{}^{40} \quad [\mathrm{erg \, g^{-1} \, s^{-1}}] \quad (\text{if } T_8 \approx 1)$$

Clayton

47

Does ^{28}Si follow the same scenario?

$^{28}Si + ^{28}Si \rightarrow ^{56}Fe$?

C+C 6×10^8 K
O+O 10^9 K

No ! Coulomb barrier becomes extremly high; another nuclear reaction takes place

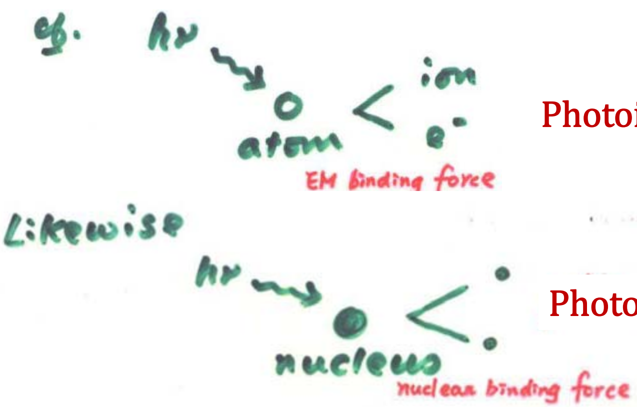

Photoionization

Photodisintegration

48

For example, $^{16}O + \alpha \leftrightarrow {}^{20}Ne + \gamma$
If $T < 10^9$ K $\rightarrow$
but if $T \geq 1.5 \times 10^9$ K (in radiation field) $\leftarrow$

So ^{28}Si disintegrates at $\approx 3 \times 10^9$ K to lighter elements
(then recaptured …)
Until a nuclear statistical equilibrium is reached

But the equilibrium is not exact
→ pileup of the iron group nuclei (Fe, Co, Ni)
which can resist photodisintegration until 7×10^9 K

49

Nuclear Fuel	Process	$T_{threshold}$ (10^6 K)	Products	Energy per nucleon (MeV)
H	p-p	~4	He	6.55
H	CNO	15	He	6.25
He	3α	100	C, O	0.61
C	C + C	600	O, Ne, Na, Mg	0.54
O	O + O	1,000	Mg, S, P, Si	~0.3
Si	Nuc. Equil.	3,000	Co, Fe, Ni	<0.18

From Prialnik Table 4.1

50

$^{56}Fe + 100\ \text{MeV} \rightarrow 13\ ^{4}He + 4\,n$

If T ↑↑↑, even $^{4}He \rightarrow p^{+} + n^{0}$

So stellar interior has to be between a few T_6 and a few T_9.

Lesson: Nuclear reaction that absorb energy from ambient radiation field (in stellar interior) can lead to catastrophic consequences.

51

Alternative Energy --- Accretion Energy

Accretion Energy

$$L = \frac{GM}{R}\dot{M}$$

in terms of the Schwarzschild radius $R_S \equiv \frac{2GM}{c^2}$

$$\Rightarrow L = \left[\frac{R_S}{2R}\right]\dot{M}c^2$$

'efficiency'; ↑ as R ↓

Accretion is highly efficient onto a compact object.

52

For chemical reactions typically ~ a few eV

e.g., H_2 dissociation, $E \sim 4.48$ eV

$$\therefore \frac{4.48\,\text{eV}}{2m_p} \sim 10^{12}\,\text{erg}\,g^{-1} \rightarrow 10^{-9}\ \text{eff.}$$

For nuclear reactions typically ~ a few MeV

e.g., $4H \rightarrow He$, $E \sim 7$ MeV

$$\therefore \frac{7\,\text{MeV}}{m_p} \sim 10^{19}\,\text{erg}\,g^{-1} \rightarrow 10^{-2}\ \text{eff.}$$

For accretion process $E \sim 10^{21}\,\text{erg}\,g^{-1}$

Ex. a neutron star $R \sim 15$ km, $\frac{R_s}{2R} \sim 0.1$

Longair "High-Energy Astrophysic"

53

Time Scales

Different physical processes inside a star,
e.g., nuclear reactions (changing chemical composition) are slow (longer time scales); structural adjustments (dP/dt) take places on relatively shorter time scales.

- ✓ Dynamical timescale
- ✓ Thermal timescale
- ✓ Nuclear timescale
- ✓ Diffusion timescale

54

Dynamical Timescale

hydrostatic equilibrium $\xrightarrow{\text{perturbation}}$ motion $\xrightarrow{\text{adjustment}}$ hydrostatic equilibrium

Free-fall collapse

Equation of motion $\ddot{r} = -\frac{GM_r}{r^2} - \frac{1}{\varrho}\frac{dP}{dr}$

Near the star's surface $r = R, M_r = M$, so $\ddot{R} = -\frac{GM}{R^2} - \frac{1}{\varrho}\frac{dP}{dR}$

Free-fall means pressure ≪ gravity, so $\ddot{R} \approx -\frac{GM}{R^2}$

Assuming a constant acceleration $R = -(\ddot{R}/2)\,\tau_{\text{ff}}^2$, so

$$\tau_{\text{ff}} = (2R^3/GM)^{1/2} = \frac{1}{\left(\frac{2}{3}\pi G\bar{\rho}\right)^{1/2}} \approx 0.04\left(\frac{\rho_\odot}{\bar{\rho}}\right)^{1/2} \text{[d]}$$

55

Stellar Pulsation

The star pulsates about the equilibrium configuration

→ same as dynamical timescale

$$\tau_{\text{pul}} \propto 1/\sqrt{\bar{\rho}}$$

Propagation of Sound Speed (pressure wave)

Pressure induced perturbation,

$$R/\tau_{\text{ff}}^2 = -\frac{\ddot{R}}{2} = \frac{GM}{R^2} + \frac{1}{\varrho}\frac{dP}{dR} \approx \frac{1}{\varrho}\frac{dP}{dR} \approx \frac{1}{\varrho}\frac{P}{R}$$

so $\frac{R}{\tau_{\text{ff}}} \approx \sqrt{\frac{P}{\rho}} \approx c_s$ (sound speed) $\propto \sqrt{T}$ (for ideal gas)

$$\tau_s \approx \frac{R}{c_s}$$

In general, $\tau_{\text{dyn}} \approx \frac{1}{\sqrt{G\bar{\rho}}} \approx \frac{1.6\times10^{15}}{\sqrt{n}}$ [s] $= 1000\sqrt{\left(\frac{R}{R_\odot}\right)^3\left(\frac{M_\odot}{M}\right)}$ [S]

56

Thermal Timescale

Kelvin-Helmholtz timescale (radiation by gravitational contraction)

$$E_{\text{total}} = E_{\text{grav}} + \text{E}_{\text{thermal}} = \frac{1}{2} E_{\text{grav}} = -\frac{1}{2}\,\alpha\, GM^2/R$$

This amount of energy is radiated away at a rate L, so timescale

$$\tau_{\text{KH}} = \frac{E_{\text{total}}}{L} = \frac{1}{2}\alpha\, GM^2/RL$$
$$= 2 \times 10^7\, M^2/RL \quad [\text{yr}] \text{ in solar units}$$

$$\tau_{\text{KH}} \approx 2 \times 10^7 \left(\frac{M}{M_\odot}\right)^2 \left(\frac{R_\odot}{R}\right)\left(\frac{L_\odot}{L}\right) \; [\text{yr}]$$

57

$M = 1\,\mathcal{M}_\odot, R = 1\ \text{pc}$	$M = 1\,\mathcal{M}_\odot, R = 1\,\mathcal{R}_\odot$
$\tau_{\text{dyn}} \approx 1.6 \times 10^7\ \text{yr}$	$\tau_{\text{dyn}} \approx 1.6 \times 10^3\ \text{s} \approx 30\ \text{min}$
$\tau_{\text{ther}} \approx 1\ \text{yr}$	$\tau_{\text{ther}} \approx 3 \times 10^7\ \text{yr}$

58

Nuclear Timescale

Time taken to radiate at a rate of L on nuclear energy

$4\ {}^{1}H \rightarrow {}^{4}He\ (Q = 6.3 \times 10^{18} \text{erg/g})$

$$\tau_{\text{nuc}} = \frac{E_{\text{nuc}}}{L} = 6.3 \times 10^{18}\,\frac{M}{L}$$

$$\tau_{\text{nuc}} \approx 10^{11}\left(\frac{M}{M_{\odot}}\right)\left(\frac{L_{\odot}}{L}\right)\ \text{[yr]}$$

From the discussion above, $\tau_{\text{nuc}} \gg \tau_{\text{KH}} \gg \tau_{\text{dyn}}$

59

Main-Sequence Lifetime of the Sun

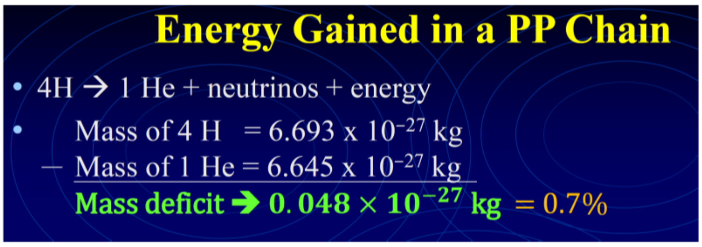

$M_{\odot} \approx 2 \times 10^{33}$ [g]

$L_{\odot} \approx 4 \times 10^{33}$ [ergs/s]

Fusion efficiency

Nuclear physics

Stellar physics

$$\tau_{\odot}^{\text{MS}} \approx M_{\odot}\frac{(0.007)(0.1)\,c^2}{L_{\odot}} = 3.15 \times 10^{17}\,\text{[s]} = 10^{10}\ \text{[yr]}$$

Given $L_{\text{MS}}/L_{\odot} \approx (M/M_{\odot})^4 \rightarrow \tau^{\text{MS}} \approx 10^{10}\,(M_{\odot}/M)^3$ [yr]

60

Diffusion Timescale

Time taken for photons to randomly walk out from the stellar interior to eventual radiation from the surface

$r_e = \frac{1}{4\pi\epsilon_0}\frac{e^2}{m_e c^2}$ ("classical" radius of the electron)

$\sigma_{\mathrm{Thomson}} = \frac{8\pi}{3} {r_e}^2 = 6.6525 \times 10^{-29}$ [m^2] for interactions with photon energy $h\nu \ll m_e c^2$ (electron rest energy)

Thus, mean free path $\ell = 1/(\sigma_T n_e)$, where for complete ionization of a hydrogen gas, $n_e = M/(m_p R^3)$.

So, $\ell \approx m_p R^3/\sigma_T M = 4$ [mm] for the mean density.

At the core, it is 100 times shorter.

$\tau_{\mathrm{dif}} \approx 10^4$ [yr] (Exercise: Show this.)

61

For an isotropic gas

$$P = \frac{1}{3}\int_0^\infty p\, v_p\, n(p)\, dp$$

- p and v_p: relativistic case
- $n(p)$: particle type & quantum statistics

For a photon gas, $p = h\nu/c$, so

$$P_{rad} = \frac{1}{3}\int_0^\infty h\nu\, n(\nu)\, d\nu = \frac{1}{3}u = \frac{1}{3}aT^4\,,$$

$$a = 7.565 \times 10^{15}\ \mathrm{ergs\ cm^{-3}\ K^{-4}}$$

62

Radiation Pressure

$P_{\text{total}} = P_{\text{radiation}} + P_{\text{gas}}$

Since $P_{\text{rad}} \sim T^4 \sim M^4/R^4$

But $P_{\text{tot}} \sim M^2/R^4$

➔ $P_{\text{rad}}/P_{\text{tot}} \sim M^2$

So the more massive of a star, the higher relative contribution by radiation pressure (and γ decreases to 4/3.)

63

When P_{rad} dominates

$$\mathcal{F} = \frac{-d\,P_{\text{rad}}/dr}{\kappa\rho} = \frac{4ac}{3}\,T^3\,\frac{dT}{dr} = \frac{L}{4\pi r^2}$$

$$\frac{d\mathrm{P}_{\text{rad}}}{dr} \sim \frac{\kappa\rho}{c}\,\frac{L}{4\pi r^2}$$

On the other hand, by definition

$$\frac{dP_{\text{tot}}}{dr} = -\rho\,\frac{Gm}{r^2}$$

$$\Rightarrow \frac{d\mathrm{P}_{\text{rad}}}{dP_{\text{tot}}} = \frac{\kappa L}{4\pi c G m}$$

64

Toward the outer layers, both $P_{\rm gas} \searrow$ **and** $\mathrm{P_{rad}} \searrow$**, so** $P_{\rm tot} \searrow\searrow$**, and** $dP_{\rm tot} > dP_{\rm rad}$**. This leads to**

$$\kappa L \leq 4\pi c G m$$

At the surface, $m = M, P = 0$**, it is always radiative, so**

$$L < \frac{4\pi c G M}{\kappa}$$

This is the Eddington luminosity limit = Maximum luminosity of a celestial object in balance between the radiation and gravitational force.

Numerically,

$$L_{Edd}/L_{\odot} = 3.27 \times 10^4 \ \mu_e \, M/M_{\odot}$$

For X-ray luminosity, scattered by electrons in an optically thin gas, $L_X < 10^{38}$ erg sec^{-1}

65

Eddington limit is the upper limit on the luminosity of an object of mass M**,** $L \leq \left(\frac{4\pi G m_p}{\sigma_T}\right) M$

$$\equiv L_{\rm Edd} \approx 10^{38} \ {}^{M}/_{M_{\odot}} \ [\mathrm{erg\,s^{-1}}]$$

For 1 $M_{\odot}$, $L_{\rm Edd} \approx 5 \times 10^4 L_{\odot}, M_{\rm bol} = -7.0$
For 40 $M_{\odot}$, $M_{\rm bol} = -11.0$

Eta Carina, $L \approx 5 \times 10^6 L_{\odot}$, $M_{\rm bol} = -11.6$, $M \approx 120\ M_{\odot}$

66

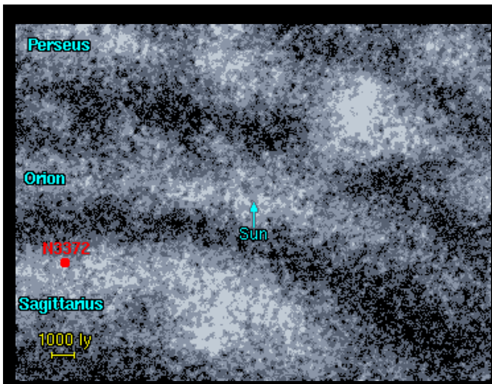

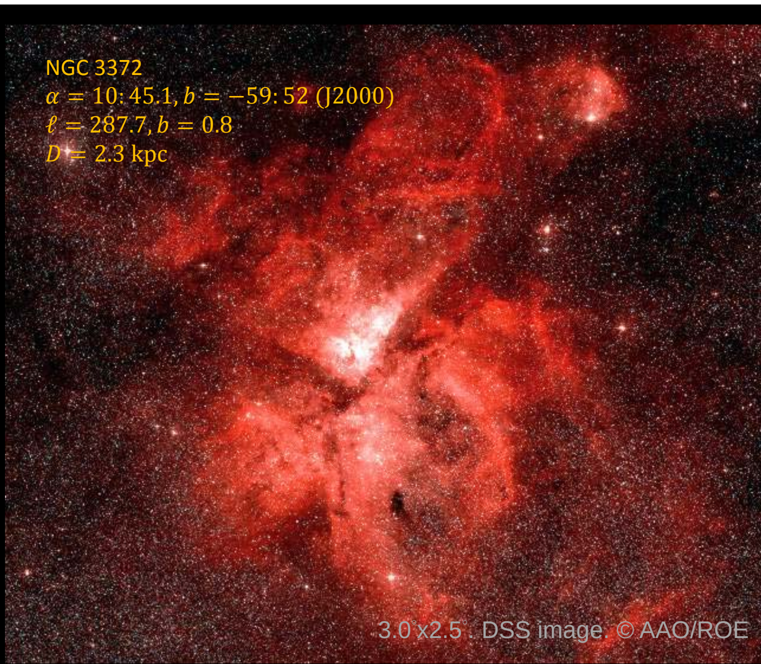

http://www.atlasoftheuniverse.com/nebulae/ngc3372.html

67

In general,

$$L_{Edd} \simeq 3.2\times10^{4}\ \frac{M}{M_\odot}\ \frac{\kappa_{e}}{\kappa}\ [L_\odot]$$

inequality is violated

L_{Edd} can be exceeded if

① $L \uparrow\uparrow$, e.g., intense thermonuclear burning

② $\kappa \uparrow\uparrow$, e.g. H or He ionization

⇒ Hydrostatic equilibrium can no longer maintained

∴ need a different heat transfer mechanism

68

Comparison of 1, 5, and 25 $\mathcal{M}_{\odot}$ stars

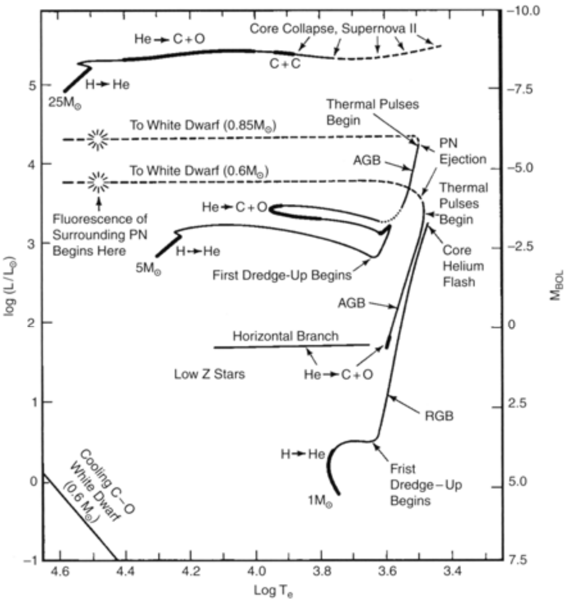

Evolutionary tracks of theoretical model stars in the HR diagram (Iben, 1985)

69